Korean J. Chem. Eng., **20**(2), 365-374 (2003)

Adsorption Characteristics of 2,4-Dichlorophenoxyacetic Acid and 2,4-Dinitrophenol in a Fixed Bed Adsorber

Sung Yong Cho†, Sook Jin Kim*, Tae Young Kim*, Hee Moon and Seung Jai Kim***

RRC for Photonic Materials and Devices, *Department of Environmental Engineering,
**Faculty of Applied Chemistry, Chonnam National University, Gwangju 500-757, Korea
(*Received 4 May 2002 • accepted 8 August 2002*)

Abstract−The influence of temperature and initial pH of aqueous solution on adsorption has been discussed in detail using the Sips equation. Single-component adsorption equilibria of 2,4-D and 2,4-DNP dissolved in water have been measured for three kinds of GACs (F400, SLS103, and WWL). For 2,4-D, the magnitude of adsorption capacity was in the order of F400>SLS103>WWL, and that for 2,4-DNP was SLS103>F400>WWL. These results may come from the effects of the pore size distribution, surface area, surface properties, and difference in adsorption affinity. Kinetic parameters were measured in a batch adsorber to analyze the adsorption rates of 2,4-D and 2,4-DNP. The internal diffusion coefficients were determined by comparing the experimental concentration curves with those predicted from surface diffusion model (SDM) and pore diffusion model (PDM). The linear driving force approximation (LDFA) model was used to simulate isothermal adsorption behavior in a fixed bed adsorber and successfully simulated experimental adsorption breakthrough behavior under various operation conditions. Efficiency of desorption for 2,4-D and 2,4-DNP was about 80% using distilled water at pH of 6.

Key words: Adsorption, Desorption, 2,4-Dichlorophenoxyacetic Acid, 2,4-Dinitrophenol, Equilibrium, Fixed Bed

INTRODUCTION

Environmental contamination by toxic xenobiotic chemicals is a serious worldwide problem. These contaminants originate predominantly from agricultural and industrial sources [Vroumsia et al., 1999]. Among the numerous agrochemicals in use today, 2,4-dichlorophenoxyacetic acid (2,4-D), a member of the phenoxy herbicide group, has been widely applied to control broad leaf weeds [Mangat and Elefsiniotis, 1999].

2,4-Dinitrophenol (2,4-DNP) is used in the manufacture of dyes and wood preservatives and as a pesticide. It is also used as an indicator for the detection of potassium and ammonium ions. 2,4-DNP exists as yellowish crystals, is slightly soluble in water, and is volatile with steam [The Merck Index, 1989].

Various treatment techniques have been employed to treat the wastewater, including precipitation, adsorption, ion exchange, and reverse osmosis [Chen and Wang, 2000]. Among them, adsorption onto solid adsorbents has great environmental significance, since it can effectively remove pollutants from both aqueous and gaseous streams. In wastewater treatment, activated carbon is a powerful adsorbent because it has a large surface area and pore volume, which remove liquid-phase contaminants, including organic compounds, heavy metal ions and coloring matters [Noll et al., 1992; Hsieh and Teng, 2000]. The characteristics, pH, and temperature of wastewater are likely to vary with time, so design of a suitable adsorption system is not that simple. In order to design effective activated carbon adsorption units and to develop mathematical models which can accurately describe their operation characteristics, sufficient information on both the adsorption and the desorption of individual pollutants under different operating conditions is required [Khan et al., 1997].

The main purpose of this work is to select a proper adsorbent for the elimination of 2,4-D or 2,4-DNP from its aqueous solution, and to study its adsorption characteristics experimentally as well as theoretically, in a fixed bed.

THEORETICAL APPROACH

1. Adsorption Equilibrium

Adsorption mechanisms are so complicated that no simple theory can adequately explain adsorption characteristics adequately. Many expressions have been reported which describe the equilibrium relationship between the adsorbate and the adsorbent [Khan et al., 1997]. Some of the well-known adsorption isotherms for single component systems are listed in Table 1.

1-1. Effect of Initial pH

The surface heterogeneity and chemical nature of the adsorbent surface are important factors for the determination of the influence of pH on the adsorption of single-component systems. In general, high pH depresses the equilibrium amount adsorbed, but neutral salt addition to the adsorbate solution increases adsorption amounts.

Table 1. Various isotherm models for single component system

Isotherm	Model equations	Parameters
Langmuir	$q=\frac{q_m bC}{1+bC}$	q_m, b
Freundlich	$q=kC^{1/n}$	K, n
Sips	$q=\frac{q_m bC^{1/n}}{1+bC^{1/n}}$	q_m, b, n

†To whom correspondence should be addressed.
E-mail: syc@chonnam.ac.kr

Table 2. Properties of adsorbents

Physical properties	Unit	F400	SLS103	WWL
Type	-	Coal-based	Coconut-based	Coal-based
Particle diameter	mm	0.37-0.54	0.37-0.54	0.37-0.54
Particle density	kg/m^3	682	880	707
Particle porosity	-	0.62	0.47	0.57
BET surface area	m^2/g	800	1040	670
Micropore area	m^2/g	490	930	360
Average pore diameter	Å	19.02	15.11	15.44

Each experimental equilibrium data can be plotted in terms of the Sips equation to obtain the pH dependent parameters, q_m and b.

The Sips equation of pH dependency is

$$q = \frac{q_m b C^{1/n}}{1 + b C^{1/n}} \quad (1)$$

The maximum adsorption amount q_m, the affinity constant b, and the exponent Z take the following form:

$$q_m = q_{m0} \exp(\alpha \cdot Z) \quad (1\text{-}1)$$

$$b = b_o \exp(-\beta \cdot Z) \quad (1\text{-}2)$$

$$Z = \frac{1}{pH} - \frac{1}{pH_m} \quad (1\text{-}3)$$

Here, b_o is the adsorption affinity constant at mean pH, pH_m. α and β are parameters of the pH dependent Sips equation.

2. Fixed Bed

It is assumed that adsorption occurs instantaneously and equilibrium is established between adsorbates in the fluid and on the surface of adsorbents. The driving force is the concentration gradient of the adsorbate between liquid bulk and pore walls. The adsorbed species then diffuse into the pores in the adsorbed state. Provided that surface diffusion is dominant, the following equation can be used to describe the rate of adsorption for a spherical particle as [Kim et al., 2001]

$$\frac{\partial q}{\partial t} = \frac{3 k_f}{R \rho_p}(C - C_s) = k_s(q_s - q) \quad (2)$$

The mass balance equation in the column and the relevant initial and boundary conditions are

$$-D_L \frac{\partial^2 C_i}{\partial z^2} + \frac{\partial \nu C_i}{\partial z} + \frac{\partial C_i}{\partial t} + \frac{1-\varepsilon_b}{\varepsilon_b}\frac{\partial q_i}{\partial t} = 0 \quad (3)$$

$$C_i(z, t=0) = 0 \quad (4)$$

$$D_L \left.\frac{\partial C_i}{\partial z}\right|_{z=0} = -\nu(C_i|_{z=0} - C_i|_{z=0}) \quad (5)$$

$$\left.\frac{\partial C_i}{\partial z}\right|_{z=L} = 0 \quad (6)$$

EXPERIMENTAL

The adsorbents used in this study were granular activated carbon (GAC) F400, SLS103 and WWL manufactured by Calgon, Samchully and Union Carbon Co., respectively. GAC was sieved into a narrow range of particle sizes (0.055-0.065 cm in diameter.), and washed with distilled water several times to remove impurities. The GACs were then stored in a sealed bottles with silica gel to prevent the readsorption of moisture. The physical properties of F400, SLS103 and WWL are listed in Table 2, and the physical properties of 2,4-D and 2,4-DNP are shown in Table 3.

Table 3. Properties of adsorbates used in this study

Compound	Structure	Mw	Water solubility (mg/*l*)	pKa (at 298.15 K)
2,4-D	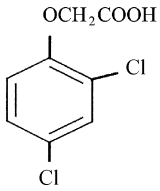	221.04	1,072 (298.15 K)	2.8
2,4-DNP	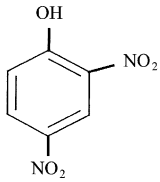	184.11	<1,000 (292.65 K)	4.0

1. Isotherm Test

Adsorption experiments were conducted by contacting a volume of solution with a carefully weighed amount of GAC in a conical flask. The amounts of GAC were varied (0.001-0.25 g), and the volume of the solution was 200 ml. The flasks were shaken for seven days to provide enough time to reach equilibrium between the solid and liquid phase. Prior to analysis of the sample taken from the flask, it was filtered to remove suspended carbon particles. Concentrations of 2,4-D and 2,4-DNP in the solution were determined using UV spectrophotometer (Shimadzu 1601) at 284 nm and 325 nm, respectively. The amount of 2,4-D and 2,4-DNP adsorbed onto the GAC at equilibrium was calculated from the following mass balance equation.

$$q = (C_i - C)\frac{V}{W} \quad (7)$$

Here q is the equilibrium amount adsorbed on the adsorbent (mol/kg), C_i is the initial concentration of bulk fluid (mol/m^3), C is the equilibrium concentration of the solution (mol/m^3), V is the volume of solution (m^3), and W is the weight of adsorbent (kg).

In this study, three isotherm models--Langmuir, Freundlich, and Sips-- were used to correlate our experimental equilibrium data. Langmuir and Freundlich equations have two parameters and the Sips equation has three parameters. To find the parameters for each

adsorption isotherm, the linear least square method and the pattern search algorithm (NMEAD) were used. The value of the mean percentage error has been used as a test criterion for the fit of the correlations. The mean percent deviation between experimental and predicted values is as follows:

$$\text{Error}(\%) = \frac{100}{N}\sum_{k=1}^{N}\left[\frac{|q_{exp,k} - q_{cal,k}|}{q_{exp,k}}\right] \quad (8)$$

2. Kinetic and Column Test

Adsorption experiments were conducted in a batch adsorber with four baffles. The rotor speed was kept at approximately 400 rpm, so that the external mass transfer resistance should be negligible. All runs were carried out at a temperature of 25 °C.

The column tests were carried out in a water-jacketed pyrex column with inside diameter and length of 1.5 and 44 cm, respectively. The column was packed with beads to distribute the solution uniformly. The activated carbon with known weight dry was put into the column. Distilled water was pumped into the column from the bottom to remove air bubbles and to rinse the carbon. In adsorption cycle, 2,4-D or 2,4-DNP solution were continuously fed to the top of the column until the column was saturated with the feed 2,4-D or 2,4-DNP solution. The saturated column was then regenerated with distilled water. The column temperature for all the column tests was maintained at 25±1 °C. The effluent samples were collected intermittently by a fraction collector and the concentration was measured by the UV spectrophotometer (Shimadzu 1601).

RESULTS AND DISCUSSION

1. Effect of Adsorbents

The surface chemistry of activated carbon and the chemical characteristics of adsorbate such as polarity, ionic nature, functional groups, and solubility in water determine the nature of bonding mechanisms as well as the extent and strength of adsorption. A variety of physicochemical forces, such as van der Waals, H-binding, dipole-dipole interactions, ion exchange, covalent bonding, cation bridging and water bridging, may be responsible for the adsorption of organic compounds on activated carbon [Zumriye and Julide, 2001].

The surface area and pore size distribution of the GACs were measured by N_2 adsorption using the BET method and the values are listed in Table 2. As shown in Table 2, the average pore diameter of F400 is 19.02 Å, while those of SLS103 and WWL are 15.11 Å and 15.44 Å, respectively. Fig. 1 shows the pore size distributions of three different adsorbents measured from desorption isotherms. According to the pore size distribution analysis, SLS103 has more micropores compared with those for F400 and WWL. Such a dif-

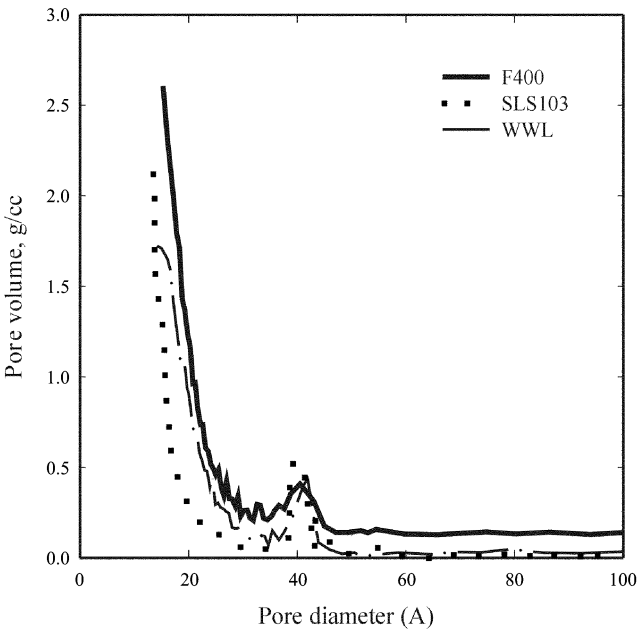

Fig. 1. Pore size distribution of three different adsorbents calculated from desorption experiments of N_2.

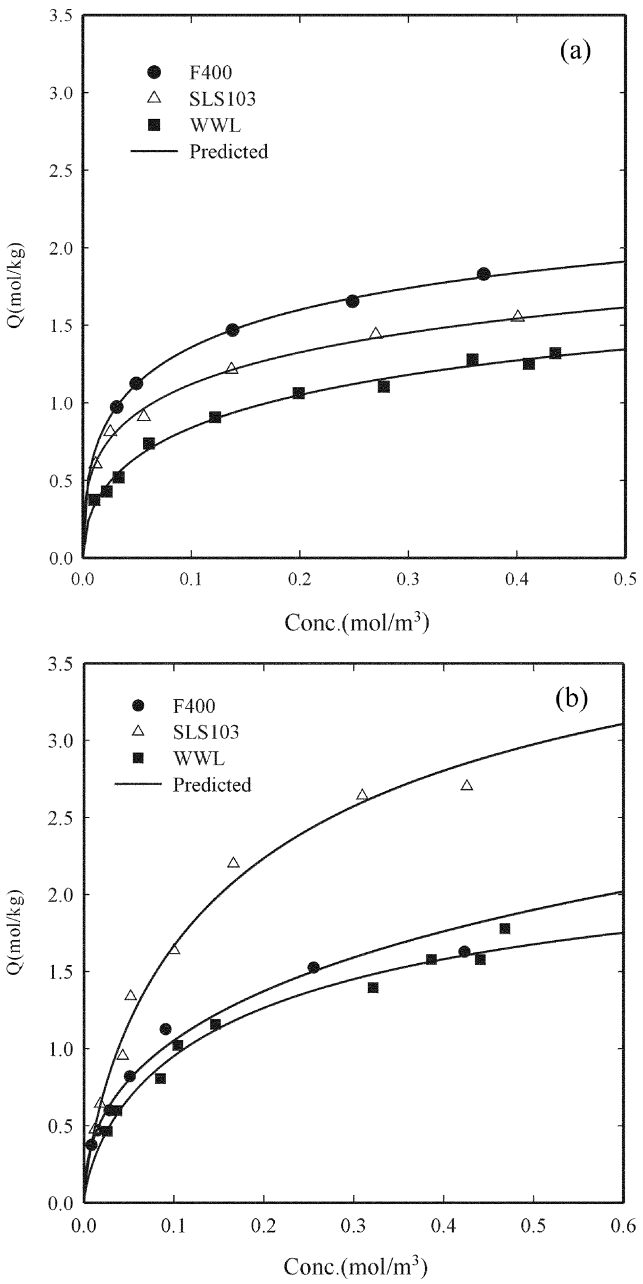

Fig. 2. Adsorption equilibrium of 2,4-D (a) and 2,4-DNP (b) onto three different adsorbents at initial pH of 3.5 and 298.15 K.

Table 4. Adsorption equilibrium constants of 2,4-D and 2,4-DNP onto F400 for different initial pHs at 298.15 K

Isotherm	Parameters	pH 3.5		pH 7.0		pH 10.0	
		2,4-D	2,4-DNP	2,4-D	2,4-DNP	2,4-D	2,4-DNP
Langmuir	q_m	1.857	1.809	0.615	0.532	0.503	0.501
	b	33.86	20.54	40.69	385.1	83.83	124.3
	Error (%)	3.111	9.786	2.937	4.844	2.710	3.432
Freundlich	k	2.369	2.542	0.771	0.754	0.598	0.697
	n	3.974	2.541	4.451	5.872	6.819	5.218
	Error (%)	1.354	5.725	2.335	5.001	2.011	2.985
Sips	q_m	3.025	6.995	0.747	0.583	0.629	0.583
	b	2.361	0.514	7.324	32.38	6.584	15.76
	n	2.164	2.163	1.623	1.616	2.156	1.619
	Error (%)	1.020	4.593	1.701	2.403	0.270	1.511

Table 5. Adsorption equilibrium constants of 2,4-D and 2,4-DNP onto SLS103 for different initial pHs at 298.15 K

Isotherm	Parameters	pH 3.5		pH 7.0		pH 10.0	
		2,4-D	2,4-DNP	2,4-D	2,4-DNP	2,4-D	2,4-DNP
Langmuir	q_m	1.384	3.247	0.646	0.569	0.631	0.552
	b	61.79	12.24	38.32	68.73	24.28	69.44
	Error (%)	8.451	7.462	3.935	1.021	2.261	1.536
Freundlich	k	2.011	4.823	0.898	0.713	0.761	0.656
	n	3.798	2.011	3.558	5.416	3.836	6.224
	Error (%)	2.990	8.980	3.428	2.570	2.203	1.775
Sips	q_m	3.458	4.466	1.393	0.584	0.753	0.643
	b	1.137	3.355	1.345	42.59	6.515	9.700
	n	2.664	1.332	2.447	1.123	1.464	1.786
	Error (%)	2.434	5.077	3.685	0.802	1.163	0.667

Table 6. Adsorption equilibrium constants of 2,4-D and 2,4-DNP onto WWL for different initial pHs at 298.15 K

Isotherm	Parameters	pH 3.5		pH 7.0		pH 10.0	
		2,4-D	2,4-DNP	2,4-D	2,4-DNP	2,4-D	2,4-DNP
Langmuir	q_m	1.431	1.770	0.571	1.182	2.183	0.542
	b	17.95	13.45	6.502	1.696	0.405	8.234
	Error (%)	7.660	5.560	1.828	5.690	3.701	7.139
Freundlich	k	1.802	2.394	0.696	1.009	0.698	0.589
	n	2.836	2.346	1.994	1.273	1.104	2.714
	Error (%)	4.797	5.679	1.693	5.638	3.943	7.531
Sips	q_m	2.460	2.593	1.012	1.144	1.453	0.463
	b	1.738	3.000	1.405	1.803	0.686	22.96
	n	1.900	1.402	1.423	0.992	0.958	0.786
	Error (%)	4.375	4.537	1.094	5.873	3.805	6.930

ference can affect the adsorption characteristics.

The adsorption isotherms of 2,4-D and 2,4-DNP onto three different adsorbents are shown in Fig. 2. As illustrated in these figures, for 2,4-D, the magnitude of adsorption capacity was in the order of F400>SLS103>WWL, and that for 2,4-DNP was SLS103> F400>WWL. This result may come from the effects of the pore size distribution and the surface area, and the surface properties. The estimated values of parameters for adsorption isotherms are summarized in Tables 4, 5 and 6.

2. Effect of Initial pH

All of the adsorption isotherms at constant pH show type I adsorption isotherm behavior, with saturation capacities depending on pH.

Figs. 3 and 4 show the experimental equilibrium adsorption isotherms obtained at different initial pHs for the adsorption of 2,4-D and 2,4-DNP onto F400. As shown in these figures, the adsorption amounts decreased with increasing initial pH of the solution, for the pH range of 3.0-10.0. The experimental data and the Sips equation (Figs. 3 and 4a) and Sips equation of pH dependency (Figs. 3 and 4b) show that the Sips model and the pH dependent Sips mod-

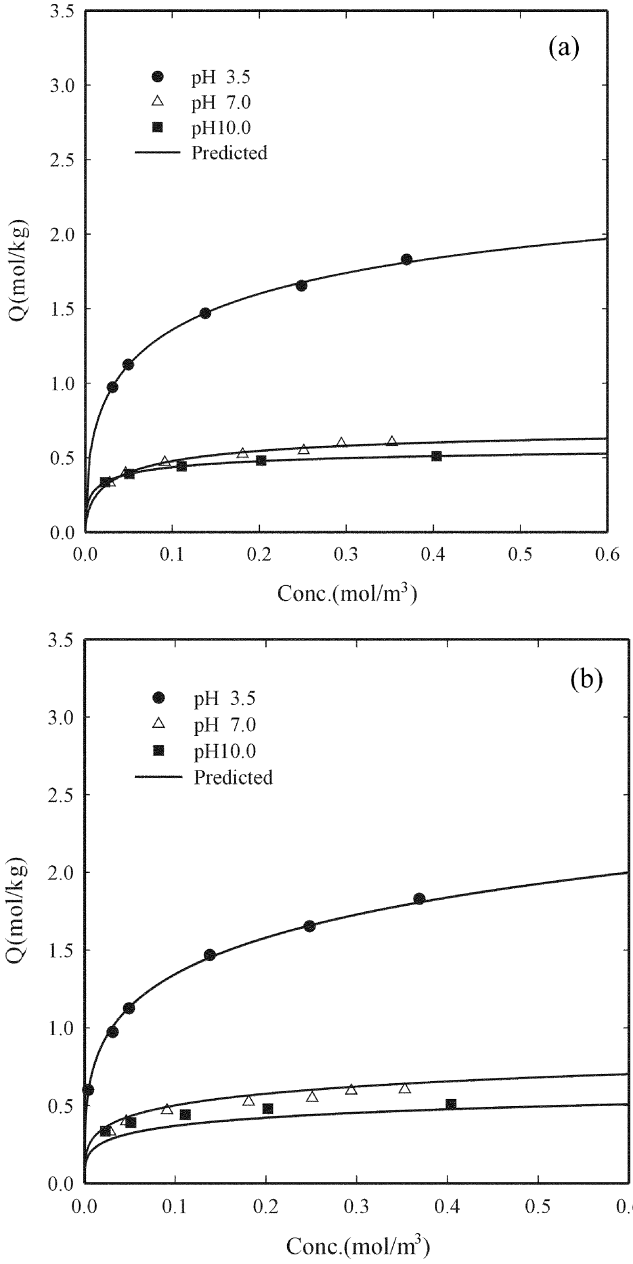

Fig. 3. Experimental data and predicted adsorption isotherms for 2,4-D-F400 system for different initial pH at 298.15 K (a: Sips Eq., b: pH dependent Sips Eq.).

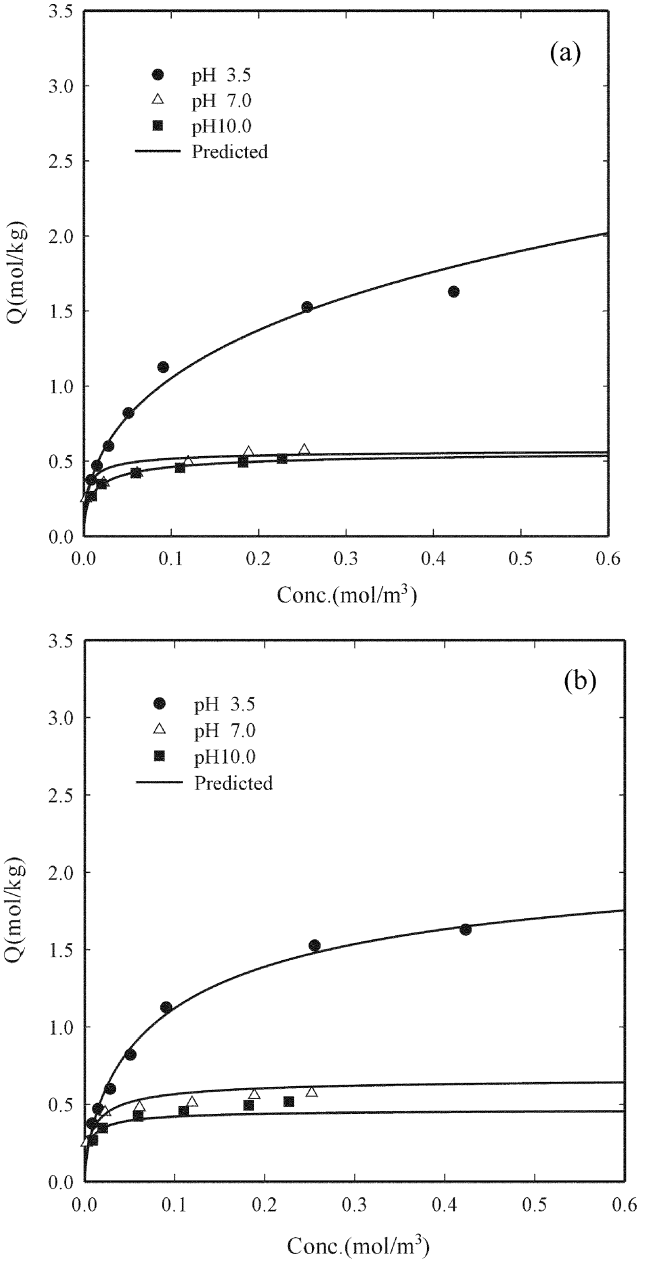

Fig. 4. Experimental data and predicted adsorption isotherms for 2,4-DNP-F400 system for different initial pH at 298.15 K (a: Sips Eq., b: pH dependent Sips Eq.).

el predict our experimental equilibrium data successfully for all of the pH conditions. The calculated parameters of Sips equation of pH dependency are listed in Table 7. Compared with those in Table 4, the percent error differences between Sips equation and the Sips equation of pH dependence are not very large. So, we could correlate single-component isotherm data by the modified Sips equation. The choice of the pH dependent function is arbitrary.

In general, the influence of pH is attributed to the electrostatic interaction between the adsorbent surface and the adsorbate molecule or ion. This suggests that effective separation could be achieved by the adjustment of pH.

2. Batch Adsorption

The adsorption on a solid surface takes place in several steps, such as external diffusion, internal diffusion, and actual adsorption. Usually, actual adsorption process is relatively fast compared to the previous two steps. Intraparticle diffusion has been usually considered as the rate-controlling step in liquid-phase adsorption. However, it is important to estimate the order of magnitude of the mass transfer coefficient. In this work, we estimated the coefficient from the initial concentration decay curve when the diffusion resistance does not prevail.

The external film mass transfer coefficient, k_f, can be obtained from the experimental concentration decay curve by plotting the $\ln(C/C_i)$ vs. t, in which time range is zero to 300 seconds [Misic et al., 1977].

$$\ln(C/C_i) = -k_f A_s t/V_s \quad (9)$$

Table 7. The calculated parameters of Sips equation of pH dependency

Adsorbates	Parameters	2,4-D	2,4-DNP
F400	q_{m0}	1.558	0.699
	a	9.219	8.494
	b	1.012	23.34
	β	3.221	11.52
	n	3.192	1.456
	Error (%)	7.931	8.237
SLS103	q_{m0}	34.30	0.823
	a	11.45	10.49
	b	0.028	23.95
	β	6.081	8.424
	n	3.779	1.122
	Error (%)	5.002	11.59
WWL	q_{m0}	1.182	340.3
	a	8.476	24.10
	b	0.795	0.002
	β	0.340	16.29
	n	2.230	2.489
	Error (%)	8.861	11.43

where V_s is the volume of solution and A_s is the effective external surface area of adsorbent particles,

$$A_s=3W/\rho_p R_p \quad (10)$$

Figs. 5 and 6 show the experimental data and model prediction of concentration profiles for the adsorption of 2,4-D and 2,4-DNP for three different adsorbents in a batch adsorber, respectively. In this study, the pore diffusion coefficient, D_p, and surface diffusion coefficient, D_s, are estimated by pore diffusion model (PDM) and surface diffusion model (SDM), respectively [Moon and Lee, 1983]. The estimated values of k_f, D_p, and D_s for 2,4-D and 2,4-DNP are listed in Table 8. Table 8 shows that the magnitude of the three estimated values, D_s is much smaller than other two. This implies that the diffusion inside a particle is a rate-controlling step.

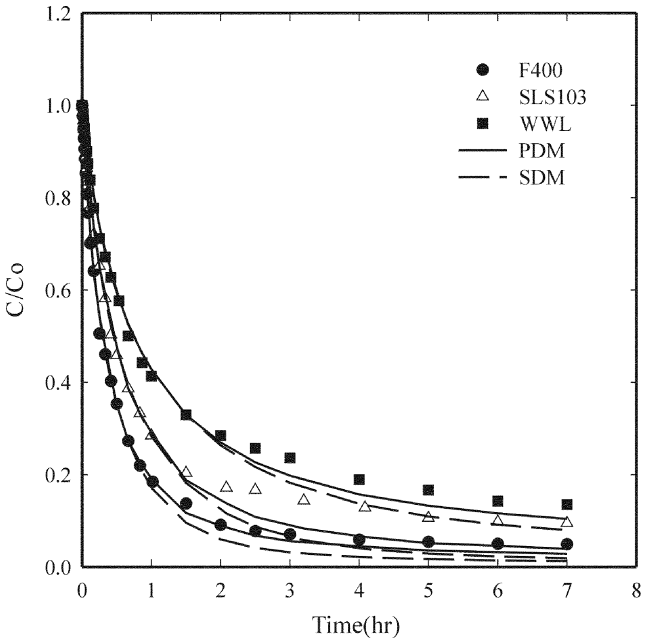

Fig. 5. Observed and predicted uptake curves of 2,4-D onto three different adsorbents at 298.15 K and initial pH of 3.5 (volume of the solution=1 L and amount of GAC=1 g).

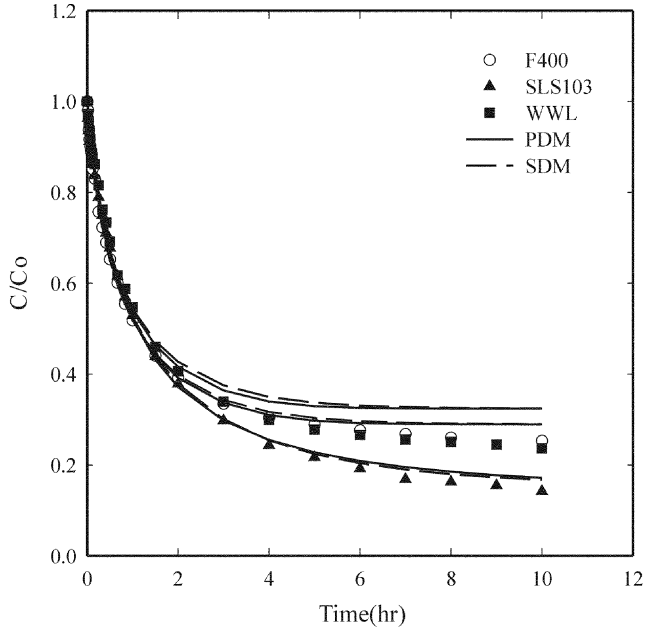

Fig. 6. Observed and predicted uptake curves of 2,4-DNP onto three different adsorbents at 298.15 K and initial pH of 3.5 (volume of the solution=1 L and amount of GAC=0.3 g).

3. Fixed Bed Adsorption

For a packed bed adsorber, the main parameters for mass transfer are the axial dispersion coefficient and the external film mass transfer coefficient. Axial dispersion contributes to the broadening of the adsorption front axially due to flow in the interparticle void spaces. Usually it comes from the contribution of molecular diffusion and the dispersion caused by fluid flow. In this study, the axial dispersion coefficient was estimated by Wakao's correlation.

$$\frac{D_L}{2\nu R_p}=\frac{20}{\xi}\left(\frac{D_m}{2\nu R_p}\right)+\frac{1}{2}=\frac{20}{Re\,Sc}+\frac{1}{2} \quad (11)$$

External film mass transfer is that by diffusion of the adsorbate molecules from the bulk fluid phase through a stagnant boundary layer surrounding each adsorbent particle to the external surface of

Table 8. Kinetic parameters onto three different adsorbents in a batch reactor

Adsorbents	Adsorbates	$k_f\times10^5$ m/sec	$D_s\times10^{13}$ m^2/sec	$D_p\times10^9$ m^2/sec
F400	2,4-D	5.00	1.90	1.42
	2,4-DNP	7.31	9.86	3.60
SLS103	2,4-D	4.17	1.85	1.50
	2,4-DNP	8.25	3.21	2.87
WWL	2,4-D	2.53	1.58	0.623
	2,4-DNP	7.23	10.4	3.69

the solid. The external film mass transfer coefficient, k_f, in a fixed bed adsorber can be estimated by Wakao and Funazkri equation [1978].

$$k_f = \frac{D_m}{2R_p}(2.0 + 1.1Re^{0.6}Sc^{0.33}) \quad (12)$$

where Sc and Re are Schmidt and Reynolds numbers, respectively. In Eqs. (11) and (12), molecular diffusion coefficients, D_m, of 2,4-D and 2,4-DNP can be calculated by Wilke-Chang equation [Reid et al., 1994].

The dynamic studies of 2,4-D and 2,4-DNP onto GAC were carried out in a fixed-bed. For these systems, the data were fitted by LDFA model. The effects of other parameters such as flow rates, and adsorbents (F400, SLS103, and WWL) on the breakthrough times are studied, and the experimental conditions are shown Table 9.

Fig. 7 shows the breakthrough curves of 2,4-D and 2,4-DNP. The breakthrough times of 2,4-D and 2,4-DNP are not different much.

Since the flow rate is an important factor in a fixed bed design, its effects were studied for different flow rate. Figs. 8 and 9 show that the breakthrough time was shorter for higher flow rate. Usually, the intraparticle diffusivity is believed to be independent of flow rate. However, the breakthrough curves were found to be steep-

Table 9. Experimental conditions for fixed bed adsorption

Variables	Unit	Experimental conditions
Bed length (L)	m	0.06-0.15
Bed diameter (D)	m	0.015
Bed density	kg/m^3	385-538
Flow rate (v)	m/s	3.77×10^{-3}-1.25×10^{-2}
Temperature	K	298.15
Initial pH	-	3.5

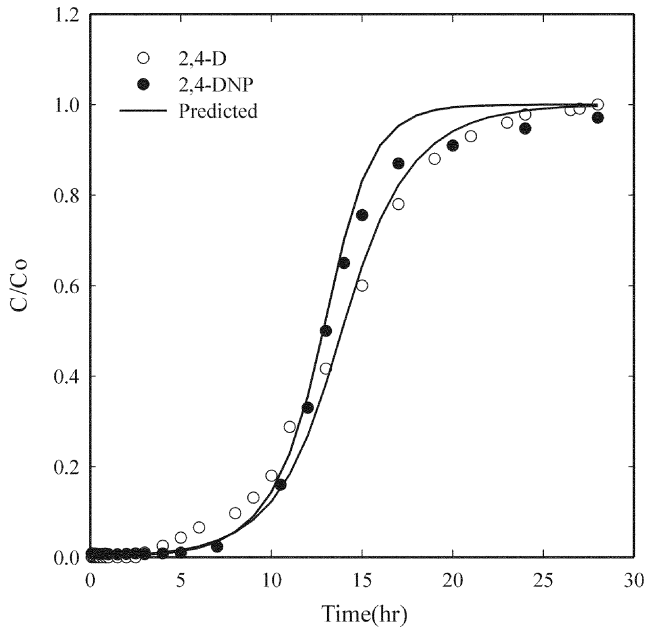

Fig. 7. Breakthrough curves of 2,4-D and 2,4-DNP on F400 (T= 298.15 K, C_0=100 mg/*l*, v=3.77×10^{-3} m/sec, L=0.10 m, and initial pH of 3.5).

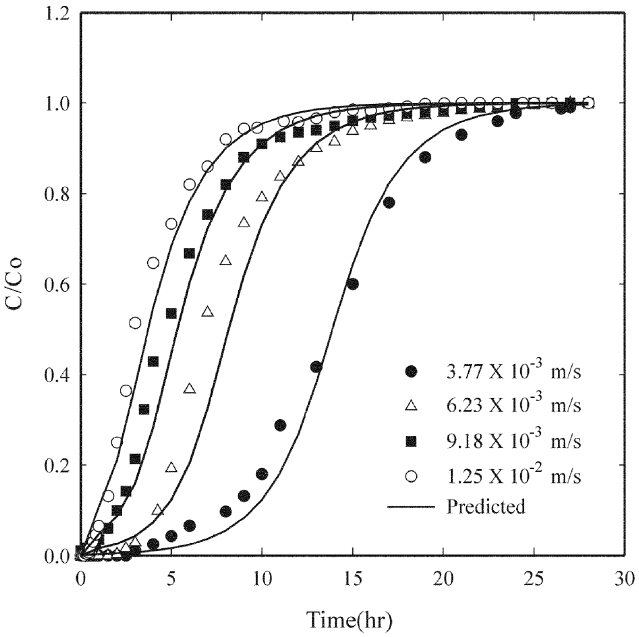

Fig. 8. Effect of flow rate on experimental results and model predictions of breakthrough curves for 2,4-D onto F400 (T= 298.15 K, Co=100 mg/*l*, L=0.10 m, and initial pH of 3.5).

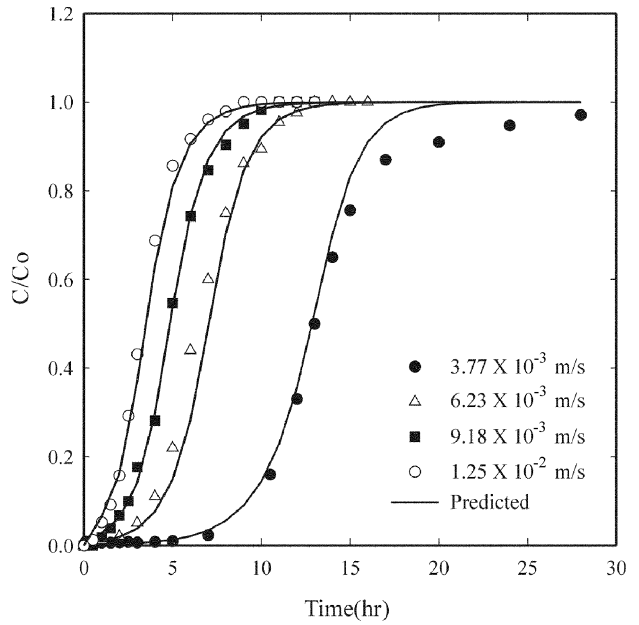

Fig. 9. Effect of flow rate on experimental results and model predictions of breakthrough curves for 2,4-DNP onto F400 (T= 298.15 K, Co=100 mg/*l*, L=0.10 m, and initial pH of 3.5).

Table 10. Estimated values of parameter for fixed-bed model simulation for different flow rates

Superficial velocity (m/sec)	$k_f\times10^5$ (m/sec)	$D_L\times10^5$ (m^2/sec)
3.77×10^{-3}	2.78	1.79
6.23×10^{-3}	3.67	2.98
9.18×10^{-3}	4.56	4.40
1.25×10^{-2}	5.43	6.00

er at higher flow rate as shown in Figs. 8 and 9. This phenomenon is attributed to the change in external film mass transfer resistance. This resistance is smaller when flow rate is higher, so that the length of mass transfer zone is reduced and a shaper breakthrough curve is generated.

Figs. 10 and 11 show the experimental data and model predictions of breakthrough curves for different GAC. The mass of adsorbent is 10 g and packed bed height of F400, SLS103, and WWL is 0.10 m, 0.12 m, and 0.14 m, respectively. This means that the bed porosity of F400 is the smallest. As shown in Fig. 2, since the adsorption capacity of 2,4-D onto F400 is greater than the other two adsorbents, the breakthrough time of 2,4-D onto F400 was longer. For 2,4-D, the breakthrough time of 2,4-DNP onto SLS103 was longer than F400 and WWL.

For the successful application of an adsorption system, an efficient regeneration of the used adsorbent is very important from the economic point of view. In general, there are many regeneration techniques such as thermal, steam, acid or base and solvent regenerations. The choice of a certain regeneration method depends upon the physical and chemical characteristics of both the adsorbate and

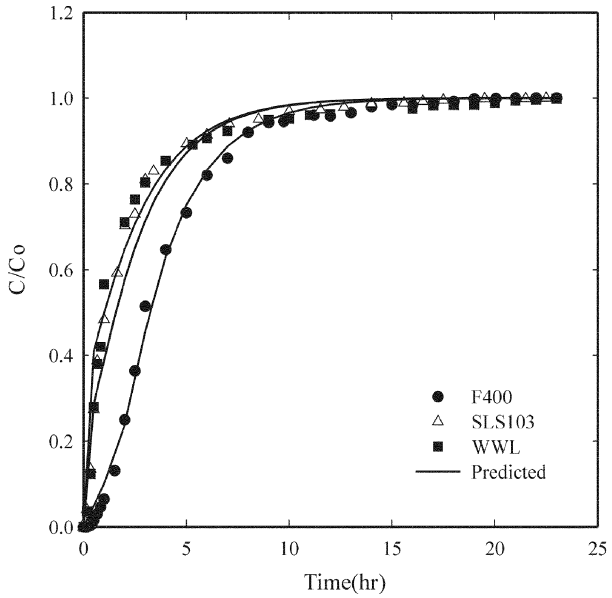

Fig. 10. Experiment data and model predictions of breakthrough curves for different GAC (Adsorbate: 2,4-D, T=298.15 K, Co=100 mg/*l*, $v=1.25\times10^{-2}$ m/sec, $pH_i=3.5$).

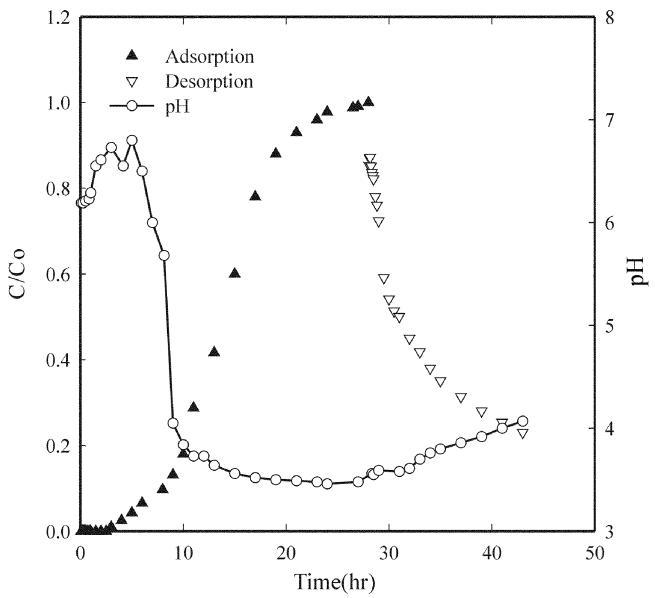

Fig. 12. pH variations during adsorption and desorption process for 2,4-D-F400 system (T=298.15 K, Co=100 mg/*l*, $v=3.77\times10^{-3}$ m/sec, L=0.10 m, $pH_i=3.5$).

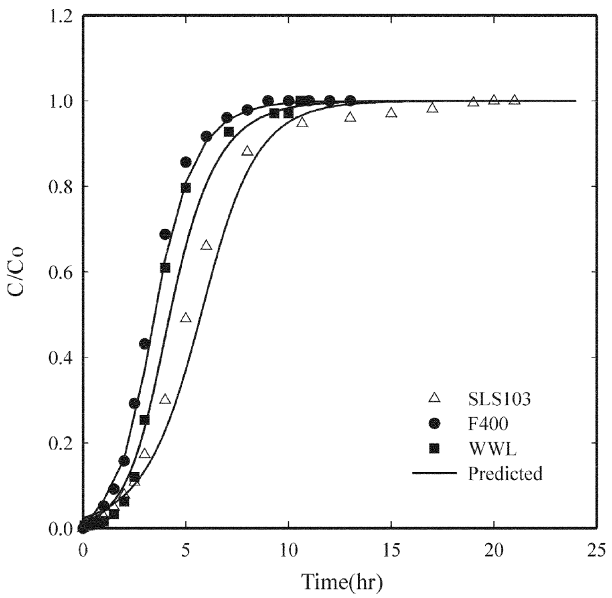

Fig. 11. Experiment data and model predictions of breakthrough curves for different GAC (Adsorbate: 2,4-DNP, T=298.15 K, Co=100 mg/*l*, $v=1.25\times10^{-2}$ m/sec, $pH_i=3.5$).

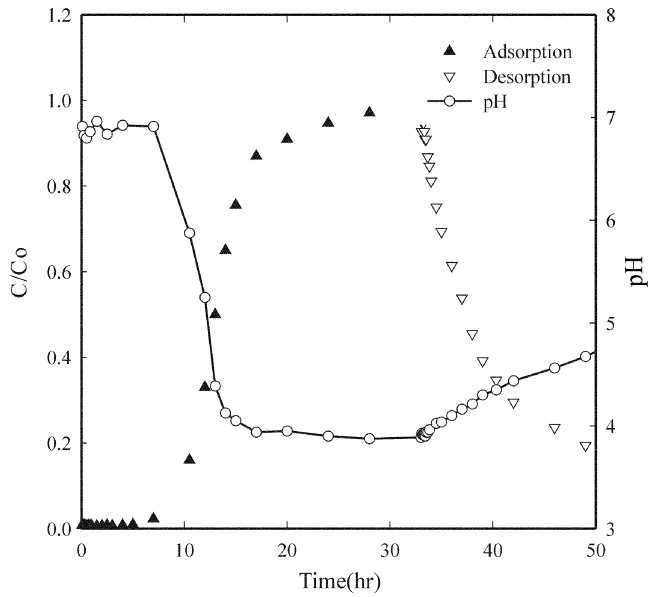

Fig. 13. pH variations during adsorption and desorption process for 2,4-DNP-F400 system (T=298.15 K, Co=100 mg/*l*, $v=3.77\times10^{-3}$ m/sec, L=0.10 m, $pH_i=3.5$).

the adsorbent. In this study, distilled water was used as desorbate for GAC. As shown in Figs. 12 and 13, desorption rate of 2,4-D and 2,4-DNP was about 80% only using distilled water of pH 6. The effluent pH decreased in the earlier adsorption stage, and then increased to influent pH as adsorption proceeded, as shown in Figs. 12 and 13. At pH 3.5 and 2,4-D concentration of 100 mg/*l*, the effluent pH decreases slowly as adsorption proceeds and reaches minimum at the end of the adsorption process, then increases slowly in the desorption process. As discussed previously, the rapid decrease of effluent pH in the earlier adsorption stage also implies that large amounts of 2,4-D and 2,4-DNP were removed by an F400 with hydronium ions on the surface functional group [Lee, 1996]. It is thought that the trailing behaviors in the breakthrough profiles are closely related to differences in adsorption capacity with pH variation of 2,4-D and 2,4-DNP solution. Since the pH varies as adsorption proceeds, and the amount of adsorption decreases as pH increases, the effect of pH should be taken into account to predict the adsorption characteristics of the adsorption column.

CONCLUSION

The adsorption isotherm of 2,4-D and 2,4-DNP onto GACs - F400, SLS103, and WWL was favorable type, and single adsorption equilibrium data could be represented by the three proposed isotherms reasonably well. Among these isotherms, for single species, Sips isotherm was used to fit the experimental equilibrium data. A Sips model with pH dependent parameters was fitted successfully with experimental data for all of the initial pHs studied. The affinity between 2,4-D and GACs was in the following order: F400>SLS103> WWL, and that for 2,4-DNP was SLS103>F400>WWL. These results may come from the effect of the pore size distribution, surface area, and surface properties of the adsorbents.

A simple dynamic model (LDFA) successfully simulated the experimental adsorption breakthrough data under various operational conditions. In particular, the adsorption capacity of F400 for 2,4-D and 2,4-DNP considerably decreased as the solution pH increased, for the pH range of 3.0-10.0. This implies that the affinity between the adsorbates and F400 depends strongly on the type of ionic forms. Though there are some deviations between experimental and simulated breakthrough curves, the adsorption method applied in this work for the treatment of coexistent ions will be very useful in predicting the adsorption behavior, especially at low pHs, which is a typical condition for aqueous solutions containing 2,4-D and 2,4-DNP.

ACKNOWLEDGMENT

This research was financially supported by the Korea Research Foundation (KRF-Y00-316).

NOMENCLATURE

A_s : surface area of the adsorbent particles [m^2]
b : isotherm parameter
C : equilibrium concentration of the solution [mol/m^3]
C_i : initial concentration of bulk fluid [mol/m^3]
C_s : saturation concentration of the adsorbate in the liquid phase [mol/m^3]
D_L : axial dispersion coefficient [m^2/sec]
D_m : molecular diffusion coefficient [m^2/sec]
D_p : pore diffusion coefficient [m^2/sec]
D_s : surface diffusion coefficient [m^2/sec]
k : isotherm parameter
k_f : film mass transfer coefficient [m/sec]
k_s : solid mass transfer coefficient [sec^{-1}]
n : isotherm parameter
pH_i : initial pH
q : equilibrium amount adsorbed on the adsorbent [mol/kg]
q_i : concentration of bulk fluid [mol/kg]
q_m : maximum adsorption capacity of adsorbent [mol/kg]
q_s : concentration at the exterior surface of the particle [mol/kg]
R_p : particle radius [m]
T : temperature [K]
t : time [sec, hr]
V : volume of solution [m^3]
v_s : superficial velocity [m/sec]
W : weight of adsorbent [kg]
z : axial distance [m]

Greek Letters

α : equilibrium constant of Sip equation of pH dependency
β : equilibrium constant of Sip equation of pH dependency
ρ_p : particle density [kg/m^3]
ε_b : bed porosity
ξ : voidage between granules (void fraction)

Abbreviation

GAC : granular activated carbon
PDM : pore diffusion model
Re : Reynolds number
Sc : Schmidt number
SDM : surface diffusion model

REFERENCES

Buckingham, J., "Dictionary of Organic Compounds," 5th Ed. and Supplements, Chapman and Hall, New York, **2**, 2275 (1988).

Chen, J. P. and Wang, X., "Removing Copper, Zinc, and Lead Ion by Granular Activated Carbon in Pretreated Fixed-bed Columns," *Sep. & Purifi. Tech.*, **19**, 157 (2000).

Hornsby, A. G., Wauchope, R. D. and Herner, A. E., "Pesticide Properties in the Environment," Springer - Verlag New York, Inc. (1996).

Hsieh, Ch. T. and Teng, H., "Influence of Mesopore Volume and Adsorbate Size on Adsorption Capacities of Activated Carbons in Aqueous Solutions," *Carbon*, **38**, 863 (2000).

Khan, A. R., Ataullah, R. and Al-Haddad, A., "Equilibrium Adsorption Studies of Some Aromatic Pollutants from Dilute Aqueous Solutions on Activated Carbon at Different Temperatures," *J. Colloid Interface Sci.*, **194**, 154 (1997).

Kim, T. Y., Kim, S. J. and Cho, S. Y., "Effect of pH on Adsorption of 2,4-Dinitrophenol onto an Activated Carbon," *Korean J. Chem. Eng.*, **18**, 755 (2001).

Kim, Y. M. and Suh, S. S., "A New Mass Transfer Model for Cyclic Adsorption and Desorption," *Korean J. Chem. Eng.*, **16**, 401 (1999).

Lee, J. W., "Seperation of Cephalosporin C in Nonionic Polymeric Resin Columns," PhD. Thesis, Department of Chemical Technology, Chonnam National University (1996).

Mangat, S. S. and Elefsiniotis, P., "Biodegradation of the Herbicide 2,4-Dichlorophenoxyacetic Acid (2,4-D) in Sequencing Batch Reactors," *Wat. Res.*, **33**, 861 (1999).

Markovska, L., Meshko, V. and Noveski, V., "Adsorption of Basic Dyes in a Fixed Column," *Korean J. Chem. Eng.*, **18**, 190 (2001).

Misic, D. M., Sudo, Y., Suzuki, M. and Kawazoe, K., "Liquid to Particle Mass Transfer in a Stirred Batch Adsorption Tank with Nonlinear Isotherm," *J. Chem. Eng. Japan*, **15**, 490 (1977).

Moon, H. and Lee, W. K., "Intraparticle Diffusion in Liquid-phase Adsorption of Phenols with Activated Carbon in Finite Batch Adsorber," *J. Colloid Interface Sci.*, **96**, 162 (1983).

Noll, K. E., Gounaris, V. and Hou, W. S., "Adsorption Technology for Air and Water Pollution Control," Lewis Publishers (1992).

Reid, R. C., Prausnitz, J. M. and Pokung, B. E., "The Properties of Gases and Liquids," McGraw-Hill Co., New York (1994).

The Merck Index, "An Encyclopedia of Chemicals, Drugs, and Biologicals," 11thed. Ed. S. Budavari. Merck and Co. Inc., Rahway, NJ (1989).

Vroumsia, T., Steiman, R., Seigle-Murandi, F. and Benoit-Guyod, J. L., "Effects of Culture Parameters on the Degradation of 2,4-Dichlorophenoxyacetic Acid (2,4-D) and 2,4-Dichlorophenol (2,4-DCP) by Selected Fungi," *Chemosphere*, **39**, 1397 (1999).

Zumriye, A. and Julide, Y., "A Comparative Adsorption/Biosorption Study of Mono- Chlorinated Phenols onto Various Sorbents," *Waste Management*, **21**, 695 (2001).